

# A Development of Recoil & Counter Recoil Motion Measurement System Using LVDT

Ju-Ho Choi, Sung-Soo Hong, and Joon Lyou

**Abstract:** This paper presents a recoil and counter recoil motion measurement system using linear variable differential transformers (LVDT). The output of the LVDT is obtained from the differential voltage of the secondary transformers. Since a transducer core is attached to the motion body, the output is directly proportional to the movement length of the core. Displacement, velocity and acceleration are measured from the LVDT. With a comparison between the measurement result and the reference value obtained by the highly accurate Vernier calipers, it is proved that the measurement system with the LVDT is applicable to the test of the moving part of the mechanism with better accuracy.

**Keywords:** linear variable differential transformer, recoil motion measurement system

## I. Introduction

This paper presents a measurement technique for the recoil & counter recoil motion of the breech in the firearms, even though there is a variety of testing mechanisms in industry. Measurement of recoil & counter recoil motion of the breech is considered important, because the performance of firearms depends on its results.

Various techniques are introduced for testing recoil & counter recoil motion, such as potentiometers using variable resistor, photographs with high speed camera, solenoid coils with magnet, an optical slit transducers with the principle of light, and LVDTs using transformer, which have advantages and disadvantages according to their applications[1].

The potentiometer technique is designed to utilize the output signal to the resistance change of the variable resistor built in the ring gear, which has some difficulties in installing the transducer on test objects. The high speed camera has some errors caused by movement of the camera due to shooting vibration and shock, and by the data processing method. In addition, the test cost tends to be higher since it requires lots of time in data processing and many rolls of expensive film.

The magnetic bar transducer provides polarity of motion direction and a more detailed phenomenon of motion vibration. On the other hand, it cannot be utilized for slow velocity movements and it is difficult to mounting.

The optical slit transducer is often used in long range recoil & counter recoil motion testing, but is limited in the high speed motion testing due to a slow response.

The LVDT is available in the measurement regardless of velocity and distance of the recoil & counter recoil motion and better accurate. LVDT mounting is easy because of the light compact size.

The scope described in this paper is as follows: the characteristic analysis of various recoil & counter recoil transducers, in particular the LVDT, the acquisition and process of measuring signals using the LVDT, the construction of the system, and finally its performance results[2].

## II. Construction of the measurement system and data processing

The measurement system of recoil and counter recoil motion consists of LVDT sensors, signal conditioner, data processor, calibrator and printer as shown in Fig. 1.

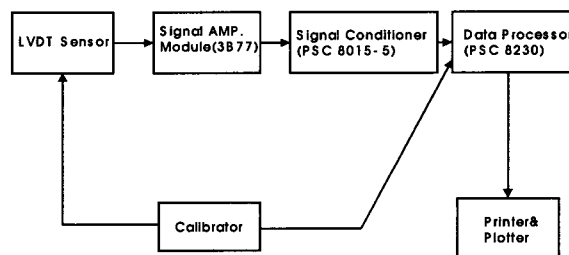


Fig. 1. Block diagram of the recoil and counter recoil motion measurement system.

### 1. LVDT transducer

By applying excitation voltage to the primary coil, the LVDT transducer structure in Fig. 2 generates output voltage corresponding to the position of the iron core. The sensing core is made of magnetic material, but the extension bar is nonmagnetic material[3][4].

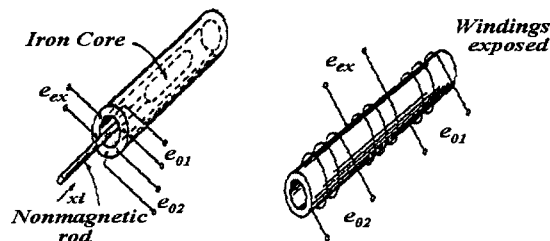


Fig. 2. LVDT transducer.

Because there is no friction, the LVDT transducer has longer life and higher reliability, since the electric part of the LVDT transducer is completely separated from the mechanical part. In addition, it provides high resolution, stable repetition

and wide application on pneumatic and hydraulic test objects.

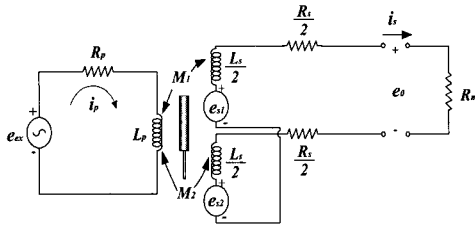


Fig. 3. Equivalent circuit of LVDT transducer.

The equivalent equations of Fig. 3 can be expressed by (1) – (4)

$$e_{ex} = L_p \frac{di_p}{dt} + R_p i_p \quad (1)$$

$$e_{s1} = M_1 \frac{di_p}{dt} \quad (2)$$

$$e_{s2} = M_2 \frac{di_p}{dt} \quad (3)$$

$$\begin{aligned} e_s &= e_{s1} - e_{s2} = (M_1 - M_2) \frac{di_p}{dt} \\ &= e_o |_{open\ circuit}. \end{aligned} \quad (4)$$

Let us define a differential operator as  $p$ , and apply  $i_p$  to (4)

$$\frac{e_o}{e_{ex}}(p) = \frac{[(M_1 - M_2)/R_p]p}{\tau_p p + 1}, \quad \tau_p \equiv \frac{L_p}{R_p}. \quad (5)$$

Such that the input resistance  $R_m$  is loaded at the output stage, the current  $i_s$  goes through  $R_m$ . The voltage equation is denoted using  $i_s$  and  $i_p$

$$e_o = (M_1 - M_2) \frac{di_p}{dt} = (M_1 - M_2) p i_p \quad (6)$$

$$\frac{e_o}{e_{ex}}(p) = \frac{d p}{d p^2 + b p + C} \quad (7)$$

$$\begin{aligned} a &= [M_1 - M_2]^2 + L_s L_p \\ b &= [L_p(R_s + R_m) + L_s R_p] \\ c &= (R_s + R_m) R_p \\ d &= R_m (M_1 - M_2) \end{aligned}$$

where if  $R_m \gg (L_s p + R_s)$ , (7) is simplified by

$$\frac{e_o}{e_{ex}}(p) = \frac{R_m (M_1 - M_2) p}{d p^2 + b p + C}. \quad (8)$$

The LVDT transducer that meets (8) always has a safe operation within the region in which the linearity of Fig. 4 is guaranteed[5].

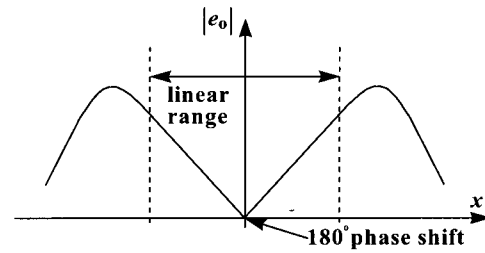


Fig. 4. Linearity of the LVDT transducer.

## 2. Transducer signal

The transducer produces output signals  $e_{o1}$  and  $e_{o2}$  when excitation voltage is applied to the primary coil. The output amplitude of  $e_{o1}$  and  $e_{o2}$  are mutually different due to the polarity of displacement in the zero position of the LVDT. The displacement quantity is obtained by the differential signal between  $e_{o1}$  and  $e_{o2}$  in the secondary coil with series opposing connection. The input signal and output signal are displayed in Fig. 5 when the iron core is held in the zero position.

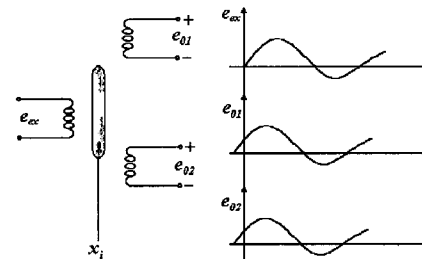


Fig. 5. Input signal waveform and output signal waveform.

## 3. Signal amplifier module (3B17)

Module 3B17 provides the blocking, amplification and filtering of signals as a signal conditioner module of single channel with wide bandwidth for LVDT interface. In the module, maximum AC excitation voltage is up to 5 Vrms at 10 kHz and signal gain is 256.

## 4. Signal conditioner (PSC 8015-5)

The existent module used in the measurement is used as a signal conditioner controlled by PC, in which maximum signal gain is 1,000, CMRR 120 dB, input impedance 10 M $\Omega$  and output impedance 1 $\Omega$ . Its signal filtering ranges from 3 Hz to 10 kHz within 0.1 % of nonlinearity error.

## 5. Data processor (PSC 8230)

The data processor based on PC is equipped with 80486 CPU at 33 MHz, 128 MB internal memory, VGA graphic card and external interfaces. Single ended inputs and differential inputs are available as input signals. In addition, it provides versatile data processing functions such as data smoothing, FFT analysis.

### ■ A/D converter

The block diagram of the A/D converter shown in Fig. 6 is composed of four modules, which provide four channels each module to measure versatile physical signals such as dis-

placement, recoil oil pressure and counter recoil oil pressure for real time acquisition. Each channel has individual programmable gain amplifier (PGA), S/H, A/D converter and memory. The A/D converter provides a 12bit resolution with a sampling rate of 1Hz~1MHz and 250Kbyte~1Mbyte per channel, and has a differential input ranged 10 mV to 100 V [6][7][8].

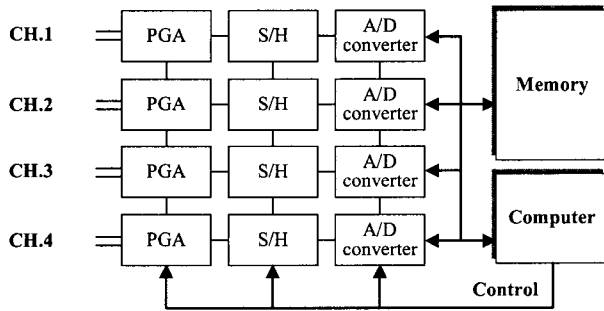


Fig. 6. Block diagram of the A/D converter.

■ Signal acquisition of the recoil & counter recoil motion

In the flow chart of signal acquisition depicted in Fig. 7, the infrared signal produced from the flame is utilized as a trigger signal when the projectile leaves the muzzle of gun. The output signal of the LVDT is converted into digital data by an A/D converter and is saved with the ratio of displacement and voltage and amplification gain for post processing.

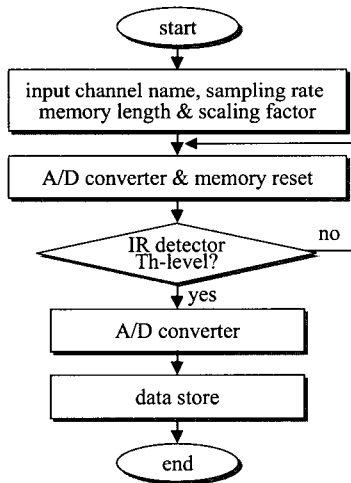


Fig. 7. Signal acquisition process of the R&CR motion.

■ Data processing

The data flow chart of Fig. 8 is described as follows: 1) the stored voltage value is multiplied by a ratio factor to gain the displacement, 2) the initial value becomes zero by adjusting the initial offset before motion, 3) the displacement data is smoothed to eliminate the noises occurring on acquisition of signal, 4) the recoil time, counter recoil time and recoil & counter recoil time are computed from the recoil motion curve, 5) finally the velocity and acceleration is obtained by differen-

tiating the displacement.

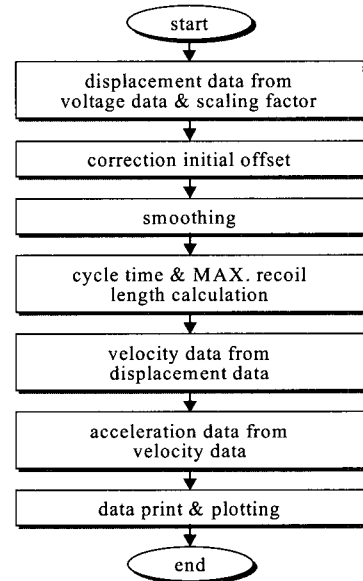
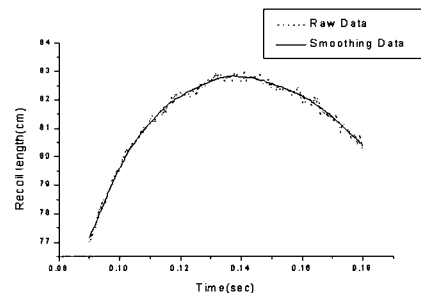


Fig. 8. Data processing flow chart of the R&CR motion.

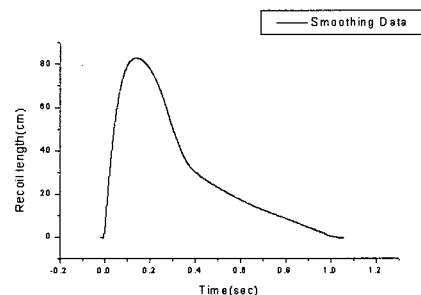
■ Displacement data smoothing

The noise included in the displacement data is reduced by filtering and smoothing. A moving window that averages the displacement data over a certain range (M=25) is used.

$$Y_s(k) = \frac{1}{M} \sum_{i=-12}^{12} Y_i(k+i) \tag{9}$$



(a) Raw data and smoothed data.



(b) Displacement.

Fig. 9. Smoothing curve of displacement.

In (9),  $k$  is the median sampling variable,  $M$  is the sampling number within the window,  $i$  is the sampling variable. In Fig. 9 (a), the dot-line indicates raw data before smoothing, and the bold line stands for the smoothed data with error reduction. The displacement data which is processed through a signal conditioner and an A/D converter with a sampling rate of 2 kHz is depicted in the second dimension of time and recoil length. Fig. 9 (b) is a displacement curve produced after smoothing which is different from Fig. 9 (a).

■ Recoil displacement and recoil & counter recoil time

In Fig. 10, which is the postprocessing flow chart of the measurement of recoil displacement and recoil & counter recoil time, the smoothed input displacement  $Y(k)$  is read until its value reaches the maximum value at step A. The maximum displacement is detected, since the input displacement at recoil time is smaller than the maximum displacement  $Y\_high$ . In step B, the time is computed until the recoil motion begins until the LVDT arrives at the maximum value. In step C, the time is calculated from the recoil time to the time of maximum displacement.

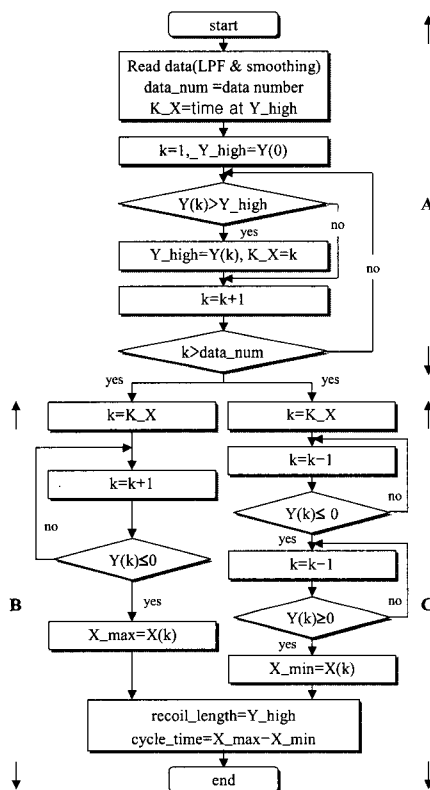


Fig. 10. Data processing flow chart of displacement and cycle time.

III. Measurement result and accuracy analysis

The transducer mounting is done more carefully so that the iron core connected to the moving part can freely move along the horizontal line. The length of extension bar made of non-magnetic stainless steel is determined depending on the maximum stroke. The LVDT transducer mounted in the moving part of the gun is shown in Fig. 11.

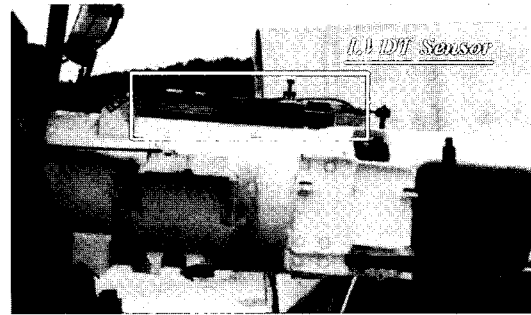


Fig. 11. Attachment of LVDT transducer.

1. Measurement result

■ Curve of displacement and velocity at the recoil & counter recoil motion

In Fig. 12, curve A indicates recoil displacement to time, and curve B represents recoil velocity to time. curve B is obtained by differentiating curve A to check out the velocity of moving object. The left vertical axis is shown in cm and the right vertical axis, mm/s in Fig. 12.

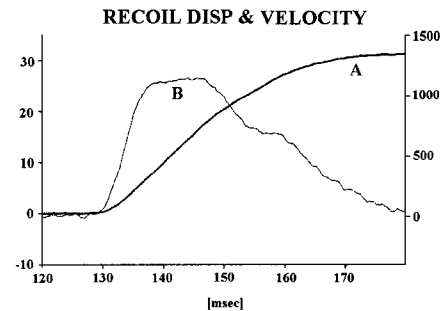


Fig. 12. Curve of recoil displacement and recoil velocity.

■ Curve of velocity and acceleration

In Fig. 13, curve B denotes velocity to time in cyclical motion. We find that recoil time and cyclical time are about 200 ms and 540 ms. The recoil velocity reaches its highest value and returns to the zero value which means the completed motion. Negative velocity of counter recoil means the opposite direction of motion. curve A is acquired by differentiating curve B. The unit of the left vertical axis and right vertical axis are mm/s and mm/s<sup>2</sup> in Fig. 13.

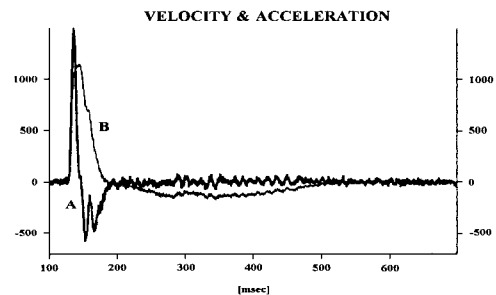


Fig. 13. Velocity and acceleration curve.

■ Displacement and acceleration curve

The curve displacement and acceleration in recoil motion is expressed in Fig. 14. The maximum recoil displacement is about 32 cm in curve B, and the maximum recoil velocity is -10 m/s in curve A. The unit of the left vertical axis and right vertical axis are cm and mm/s in Fig. 14.

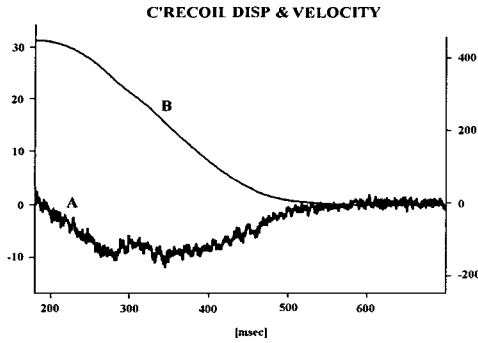
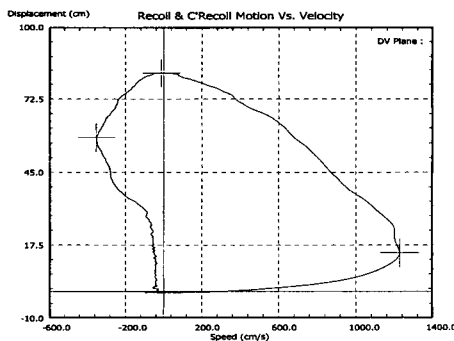


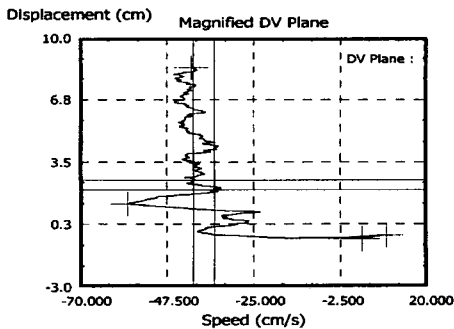
Fig. 14. Curve of counter recoil displacement and counter recoil velocity.

■ Velocity curve to displacement in counter recoil motion

Fig. 15 shows velocity function to distance at cyclical motion. The performance of the gun breech is normally evaluated by maximum recoil distance, cyclical time and velocity at the counter recoil termination. In Fig. 15, the maximum recoil velocity is about 1,227.5 cm/s, the maximum recoil distance 82.3 cm, and the average velocity -38.2 cm/s, between a recoil distance of 20.4 mm and 25.4 mm.



(a) Speed & displacement.



(b) Terminal velocity.

Fig. 15. Curve of displacement versus velocity.

2. Accuracy analysis

In the measurement system using the LVDT there remains linearity error of transducer and measurement system error.

■ Linearity error of the transducer

Transducer error is composed of linearity error, hysteric error, repetition error and transducer calibration error, which are calculated in rms. The linearity error described in the manufacturer's calibration sheet is about ±2%.

■ Property error of signal conditioner

The gain error of signal conditioner is 0.08%; gain stability 0.02% and the linearity error of amplifier 0.1% with a gain of 1,000 and temperature drift of 5μV/°C [9].

■ Accuracy analysis of the measurement system

The accuracy analysis of the measurement system with the LVDT is indicated in Table 1, which is calculated from a theoretical formula and precise measurements. The total system error within a reliability span of 2σ is computed by (10)[10].

Table 1. Error items of the R&CR motion measurement system.

Error items	Errorvalue(%)
Reading error $RE$	± 0.01
Transducer linearity error $LE_1$	± 1.0
Signal conditioner linearity error $LE_2$	± 0.1
Hysteresis error $CE_1$	± 0.03
Repeatability error $CE_2$	± 0.03
Gain setting error $CE_3$	± 0.08
Quantization error $CE_4$	± 0.02
Random error $CE_5$	± 0.01
Temperature error $EE_1$	0.0
Loading error $LE_0$	0.0

$$e_{total} = LE_0 + \sqrt{RE^2 + \left(\sum_{i=1}^2 LE_i\right)^2 + EE_1^2 + \sum_{j=1}^5 (CE_j)^2} \quad (10)$$

$$= \pm 2\% \text{ at } 2\sigma.$$

The system total error is ±2%. The performance test of the measurement system is shown in Table 2, using the Vernier calipers with an accuracy of ±0.0002%, a stroke of 40cm and an interval of 5 cm.

Table 2. Displacement measurement and error percentage.

Range (mm)	Measured Value (mm)	Error (%)	Remark
50	51.56	3.10	Vernier calipers: ±0.0002% Average Error of displacement : ±2.0% at 2σ
100	102.01	2.01	
150	150.98	0.65	
200	198.83	- 0.58	
250	247.48	- 1.00	

300	296.12	- 1.29	
350	349.24	- 0.21	
400	401.28	0.32	

#### IV. Conclusion

In this paper, a measuring technique with the LVDT is developed to measure displacement, velocity and acceleration of a moving object at low and high speeds, which is resistant to mechanical shock and has no friction compared to the existing techniques. The analysis of the performance test on the measurement system using the LVDT is summarized as follows.

The linearity and frequency response of the LVDT is obtained through various experiments, and the program for the measurement algorithm and data processing is designed to meet the measurement system with the LVDT.

The velocity and acceleration can be computed by differentiating the displacement data of the LVDT

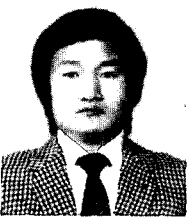
The efficiency of the test and measurement is improved a lot by the LVDT measurement system which provides easier attachment and wide-range of speed.

It is proved there is almost no difference between theoretical value and the measured value obtained by the Vernier calipers with  $\pm 0.0002$  mm.

The LVDT adaptor is designed to endure the high shock and vibration produced in the firing of the gun. The LVDT core is positioned in the same line as the moving part.

This technique is applicable to the recoil breech for the performance test since it serves real-time-data processing and high test efficiency.

We need to work on continuous study of non-linearity correction in both the static mode and dynamic mode in order to improve the accuracy of the measurement system.



#### Ju-Ho Choi

(1949) received the B. S. degree in electronics engineering from Pusan National University in 1976 and M. S. and Ph. D. degrees in electronics engineering of Chungnam National University in 1993 and 1999 respectively. He is a chief of the development of measurement technique

of Agency for Defense Development in Korea. His current research interests include instrumentation system, advanced signal processing and optical fiber communication.



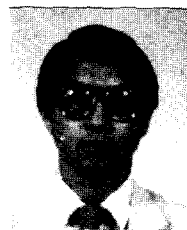
#### Joon Lyou

(1956) received the B. S. degree in electronics engineering from Seoul National University in 1978, and the M. S. and the Ph. D. degrees from Korea Advanced Institute of Science and Technology in 1980 and 1984 respectively. During the academic year 1989 to 1990

#### Reference

- [1] Aberdeen Proving, *Ground, Recoil Motion Measurement*, U.S Army TECOM, TOP 4-2-815, pp. 1~34, 1976.
- [2] Ju-Ho Choi, "A Study on the measurement technique of recoil and counter recoil motion," *ADD, TAEC-514-89003*, pp. 1~50, 1990.
- [3] P. S. Filipiski and R. Rinfret, "Calibration of a low voltage AC-DC transfer standard," in *Dig. 1998 IEEE instrumentation and measurement Technology Conf. IMTC '98*, St. Paul, MN, pp. 172-177, 1998.
- [4] E. E. Hecceg, "*Handbook of Measurement and Control, Schaevitz Engineering, Pennsauken*," N. J, pp. 3-1~3-16, pp. 14-1~14-14, 1994.
- [5] Macro Transducers Division, *LVDT Displacement Measuring Transducers*, Schaevitz Technologies, Inc. pp. 1~6, 1998. 9.
- [6] L. Ochs, "Measurement and enhancement of waveform digitizer performance," in *IEEE Int. Conv.*, Boston, MA, May., 1976.
- [7] G. N. Stenbakken and T. M. Souders, "Linear error modeling of analog and mixed-signal devices," in *IEEE Int. Test Conf.*, Nashville, TN, pp. 573-581, 1991.
- [8] Sy, Hahn, *Elsevier, Advanced Computational and Design Techniques in Applied Electromagnetic Systems*, McGraw-Hill, pp. 52~140, 1995.
- [9] Francis S. Tse & Lvan E. Morse, *Measurement and Instrumentation in Engineering*, Marcel Dekker, Inc. pp.134~147, 1989.
- [10] B. N. Taylor and G. E. Kuyatt, "*Guidelines for Evaluating and Expressing the Uncertainty of NIST Measurement Results*," NIST Technical Note 1297, pp. 1~25, 1992.

and the year 1997 to 1998, he was a visiting professor at Michigan State University and at University of California at Davis respectively. He has been a professor in the department of electronics engineering of Chungnam National University since 1984. His current research interests include estimation and identification methods for fault detection of control and instrumentation systems, and signal processing.



#### Sung-Soo Hong

He was born on November, 1955 in Jeonbuk, Korea. He received the B. S degree in electronics engineering from Sungjeon University in 1981. He has been working on the development of the technique of calibration and measurement for the weapon test in Agency for

Defense Development since 1981. He worked for one of U.S Army Proving Ground, Combat Systems Test Activity as an exchange engineer in 1987 and 1988. He has strong interest in the area of dynamic pressure calibration and measurement.